

## Thermal Budget Control for Rapid Thermal Processing Systems with Spike-Shaped Temperature Profile

Jyh-Cheng Jeng\*, Bor-Chi Lee\*\*  
An-Jhih Su\*\*, Cheng-Ching Yu\*\*

\* Department of Chemical Engineering and Biotechnology, National Taipei University of Technology, Taipei 106, Taiwan (e-mail: jcyjeng@ntut.edu.tw).

\*\* Department of Chemical Engineering, National Taiwan University, Taipei 106, Taiwan.

**Abstract:** Rapid thermal processing (RTP) systems with spike-shaped temperature profile is widely used in IC industry for providing precise thermal budgets. This thermal budget control issue gets more crucial as the technology node progressively shrinking. With its exceptionally stringent performance requirements (for example, high temperature uniformity and high temperature ramp-up/down rate), temperature control in RTP systems is a challenging task. In this study, we present the methodology of designing a control system for providing precise thermal budget. By tuning controller parameters and designing the set-point profile, the method targets thermal budget indices instead of temperature servo control. Two types of controllers, PI and PI<sup>2</sup>D, are considered. Practical issues, such as the feasibility range for temperature ramp-up/down rate and the effect of model mismatch, are also discussed. The results show the simple PI controller performs well in spike RTP systems.

**Keywords:** Thermal budget control, Rapid thermal processing, Spike annealing, PI, PI<sup>2</sup>D.

### 1. INTRODUCTION

Single wafer rapid thermal processing (RTP) is widely used in the fabrication of semiconductor devices. It has become one of the key technologies due to faster wafer processing with precise control of thermal budget. The thermal budget is an important process issue contributed from the duration and maximum of temperature beyond a specific reference value, as represented as Fig. 1. This index needs a tight process control in many processes, such as rapid thermal annealing, oxidation in semiconductor manufacturing and reflow soldering in IC packaging industry. A review of RTP control has been given by Edgar *et al.* (2000).

The traditional annealing process uses a soak-shaped temperature profile as shown in Fig. 2(a). It consists of three steps: 1) rapid heating to the desired temperature, 2) processing for a prescribed time at constant temperature, 3)

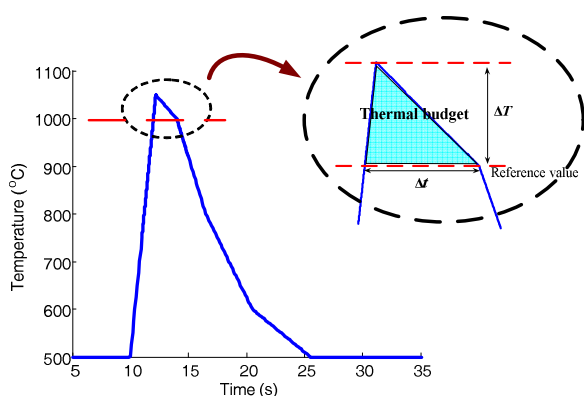


Fig. 1. Thermal budget and temperature profile for spike annealing.

rapid cooling to an ambient condition. However, as dimension keeping shrinking, the demand of shallow junctions requires very tiny and precise applied thermal energy. Therefore, the spike annealing process, as shown in Fig. 2(b), is the way to keep scaling requirements. In the spike annealing process, the second step in traditional annealing process is removed and the ramp-up/down rate of temperature trajectory is higher to prevent significant spreading of the dopant profile (Jung *et al.*, 2003). Obviously, the spike-shaped temperature control dominates the reliability and yield of semiconductor manufacturing.

In Fig. 1, the criteria of temperature trajectory for thermal budget control usually contain three indices: the duration of exceeding the reference value, the maximum temperature, and the ramp-up/down rate. As a result, a triangular-shaped set-point profile is usually applied for thermal budget control. In literature, various control methods have been proposed for RTP to follow the desired temperature trajectory. But most of them, such as Balakrishnan and Edgar (2000), Cho *et al.*, (2005), and Dassau *et al.* (2006), deal with the soak annealing process, while few methods can apply to spike annealing process (Emami-Naeini *et al.*, 2003). However,

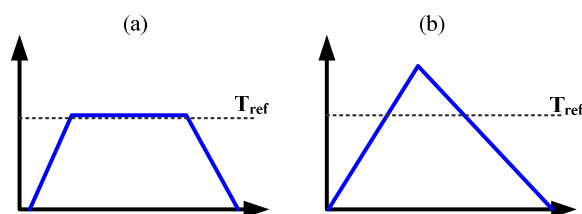


Fig. 2. Change of thermal budget shape as the line width getting narrower. (a) soak (b) spike.

achieving desired thermal budget by designing a tightened servo control system is difficult and complex due to high set-point ramp-up/down rate. Thus, in this work, we consider targeting the control performance on the indices for thermal budget instead of set-point tracking. In this way, the thermal budget can be precisely controlled and the control system design is much simpler.

## 2. RTP SYSTEM

A brief description of the single wafer RTP system and an alternative formulation of the control problem for it will be given in this section.

### 2.1 Process Description

In a RTP chamber, powers are supplied to several rings of tungsten-halogen lamps, and energy is transferred through a quartz window onto a thin semiconductor wafer via direct or reflective paths. The wafer temperature is controlled by manipulating the power sources. Assume the wafer is divided into several annual zones, and so are the cluster lamps. A physical model of the wafer temperature at different positions,  $T_i$ , is given by the energy balance equation (Huang *et al.*, 2000):

$$\rho V_i C_p \frac{dT_i}{dt} = q_i^{\text{cond}} + q_i^{\text{conv}} + q_i^{\text{rad}} + q_i^{\text{lamp}} \quad (1)$$

where subscript  $i$  is the index of annual zone with volume  $V_i$ ,  $\rho$  is the density,  $C_p$  is the heat capacity, and  $q_i^{\text{cond}}$ ,  $q_i^{\text{conv}}$ ,  $q_i^{\text{rad}}$ , and  $q_i^{\text{lamp}}$  represent the heat exchanged by conduction, convection, radiation, and heat addition from the lamp power, respectively. After linearization about an operating point, (1) can be written in deviation form as (Schaper *et al.*, 1992):

$$\tau_i \frac{d\tilde{T}_i}{dt} = -\tilde{T}_i + \sum_j K_{ij} \tilde{U}_j \quad (2)$$

Therefore, a simple first-order model could be used to describe the relationship between the lamp power from the  $j$ th zone,  $U_j$ , and the wafer temperature at the  $i$ th zone,  $T_i$ .

### 2.2 Problem Formulation for Thermal Budget Control

Although the RTP system is a multivariable process in nature, as shown in (2), the present work will focus on single-input single-output (SISO) case for simplicity. The results of SISO systems will serve as the basis of further extensions to multivariable systems. Since an approximated first-order transfer function of the process is obtained, the control designs are based on a process model of the following form.

$$G_p(s) = \frac{K}{\tau s + 1} \quad (3)$$

For the thermal budget control problem of RTP system, we formulate the control objective as two specifications: time duration beyond the reference temperature,  $\Delta t$ , and the range between the maximum temperature and the reference value,  $\Delta T$ , as shown in Fig. 1. Since constructing a control system to perfectly tracking this spike set-point is almost an impossible task, in this work, designing both the set-point profile and the controller to satisfy the specifications of thermal budget is considered. The spike-shaped set-point

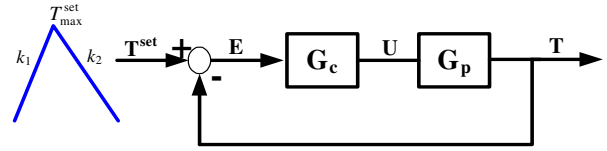


Fig. 3. Feedback control system and setpoint profile for thermal budget control.

profile can be characterized as three parameters: the ramp-up rate  $k_1$ , the ramp-down rate  $k_2$ , and the maximum value of set-point,  $T_{\text{max}}^{\text{set}}$  (see Fig. 3). The controllers considered are PI controller and PI<sup>2</sup>D controller (i.e. a PID controller with double integrators) (Huang *et al.*, 2000).

## 3. CONTROL SYSTEM DESIGN

In this section, designs of set-point profile and controllers, including PI and PI<sup>2</sup>D controllers, to satisfy the control objectives is presented.

### 3.1 Design of PI Control System

The feedback control structure is illustrated in Fig. 3. The PI controller transfer function is given as

$$G_c(s) = K_c \left( 1 + \frac{1}{\tau_i s} \right) \quad (4)$$

For simplicity, the parameter  $\tau_i$  is tuned by  $\tau_i = \tau$  to cancel the process time constant. By the final value theory, an offset appears at the steady-state when a PI controller is implemented with a ramp up input signal. The magnitude of this offset is:

$$e(\infty) = \lim_{s \rightarrow 0} sE(s) = \lim_{s \rightarrow 0} s \frac{1}{1 + G_p(s)G_c(s)} T^{\text{set}}(s) = \tau_{cl} k_1 \quad (5)$$

where  $\tau_{cl} = \tau_i / (K_c K)$  is the closed-loop time constant. A sketch of the closed-loop response is shown in Fig. 4. Let  $\bar{t} = t - t_p$  where  $t_p$  is the climax of the set-point spike, and

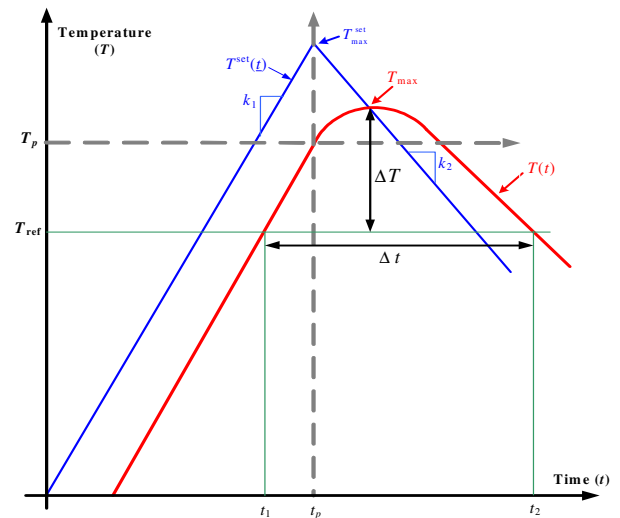


Fig. 4. Closed-loop response using PI controller (Dashed line represents the transformed coordinate).

$\bar{T} = T - T_p$ , where  $T_p = T(t=t_p)$ . In the ramp-up period, assume that the process has reached the steady-state before the rising temperature crosses the reference value  $T_{ref}$ . Therefore,  $T_p$  can be directly obtained as  $T_p = T_{max}^{set} - \tau_{cl} k_1$ , where  $T_{max}^{set}$  is the maximum value of set-point. With such a coordinate transformation, the set-point trajectory for  $\bar{t} \leq 0$  can be written as  $\bar{T}^{set}(\bar{t}) = T_{max}^{set} + k_1 \bar{t}$ , and the temperature response is given as  $\bar{T}(\bar{t}) = k_1 \bar{t}$ . On the other hand, the set-point trajectory of the ramp-down period ( $\bar{t} \geq 0$ ) is represented as  $\bar{T}^{set}(\bar{t}) = \tau_{cl} k_1 - k_2 \bar{t}$ . Consequently, the temperature response of the closed-loop system for  $\bar{t} \geq 0$  can be derived from the Laplace inversion, with the initial condition  $\bar{T}(0) = 0$ :

$$\bar{T}(\bar{t}) = L^{-1} \{ \bar{T}(s) \} = \tau_{cl} (k_1 + k_2) (1 - e^{-\bar{t}/\tau_{cl}}) - k_2 \bar{t} \quad (6)$$

With Eq.(6), the maximum temperature can be found as

$$\bar{T}_{max} = \bar{T}(\bar{t}_c) = k_1 \tau_{cl} - k_2 \tau_{cl} \ln \left( \frac{k_1 + k_2}{k_2} \right) \quad (7)$$

where

$$\bar{t}_c = \tau_{cl} \ln \left( \frac{k_1 + k_2}{k_2} \right) \quad (8)$$

Let the temperature response intersects the reference temperature at  $\bar{t}_1$  and  $\bar{t}_2$ , where  $\bar{t}_1 < \bar{t}_2$ . Notice that the value of  $\bar{t}_1$  may be negative or positive. For  $\bar{t}_1 \leq 0$ , it is obtained by equalling  $\bar{T}(\bar{t})$  to  $\bar{T}_{ref}$  as

$$\bar{t}_1 = \frac{\bar{T}_{ref}}{k_1} \quad (9)$$

For  $\bar{t}_1 > 0$ , by temperature response of (6) intersecting the reference temperature, the following equation for  $\bar{t}_1$  holds.

$$\bar{T}(\bar{t}_1) - \bar{T}_{ref} = \tau_{cl} (k_1 + k_2) (1 - e^{-\bar{t}_1/\tau_{cl}}) - k_2 \bar{t}_1 - \bar{T}_{ref} = 0 \quad (10)$$

On the other hand,  $\bar{t}_2$  is always positive and the following equation for  $\bar{t}_2$  holds.

$$\bar{T}(\bar{t}_2) - \bar{T}_{ref} = \tau_{cl} (k_1 + k_2) (1 - e^{-\bar{t}_2/\tau_{cl}}) - k_2 \bar{t}_2 - \bar{T}_{ref} = 0 \quad (11)$$

Now, the control specifications can be represented as

$$\Delta t = \bar{t}_2 - \bar{t}_1 \quad (12)$$

$$\Delta T = \bar{T}_{max} - \bar{T}_{ref} \quad (13)$$

For simplicity, assume  $k_1$  and  $k_2$  are given. Therefore, one can tune the parameter  $\tau_{cl}$  (or  $K_C$ ) and design  $T_p$  (or  $T_{max}^{set}$ ) to satisfy both specifications of  $\Delta t$  and  $\Delta T$ .

Two cases for  $\bar{t}_1$  are discussed as follows.

### Case 1: $\bar{t}_1 \leq 0$ .

First, by substituting (7), (9), (12), and (13) into (11), a nonlinear equation for  $\tau_{cl}$  is resulted. Thus,  $\tau_{cl}$  can be solved using a simple root-finding method (e.g., Newton-Raphson method). Then,  $T_p$  is calculated by  $T_p = T_{ref} + \Delta T - \bar{T}_{max}$ , and  $T_{max}^{set}$  can be obtained as  $T_{max}^{set} = T_p + \tau_{cl} k_1$ .

From (9),  $\bar{t}_1 \leq 0$  implies  $\bar{T}_{ref} < 0$ . In the limiting condition of  $\bar{t}_1 = 0$ , we have  $\bar{T}_{ref} = 0$  and, by (13),  $\bar{T}_{max} = \Delta T$ .

Therefore, the value of  $\tau_{cl}$  in this limiting case can be found from (7) as:

$$\tau_{cl}^* = \frac{\Delta T}{k_1 - k_2 \ln \left( \frac{k_1 + k_2}{k_2} \right)} \quad (14)$$

Since the closed-loop time constant  $\tau_{cl}$  must be positive,  $0 < \tau_{cl} < \tau_{cl}^*$  is thus necessary to have  $\bar{t}_1 \leq 0$ . For (11) having a solution in the interval  $0 < \tau_{cl} < \tau_{cl}^*$ , the sufficient condition is  $F_1(0) F_1(\tau_{cl}^*) < 0$ , where

$$F_1(\tau_{cl}) = \tau_{cl} (k_1 + k_2) (1 - e^{-(\bar{t}_1 + \Delta t)/\tau_{cl}}) - k_2 (\bar{t}_1 + \Delta t) - (\bar{T}_{max} - \Delta T) \quad (15)$$

### Case 2: $\bar{t}_1 > 0$ .

The procedure is similar to the previous case except the calculation of  $\bar{t}_1$ . By combining (10) and (11),  $\bar{t}_1$  can be solved as

$$\bar{t}_1 = \tau_{cl} \ln \left( \frac{\tau_{cl} (k_1 + k_2) (1 - e^{-\Delta t/\tau_{cl}})}{k_2 \Delta t} \right) \quad (16)$$

Substitute (7), (12), (13), and (16) into (11) to solve  $\tau_{cl}$ , and then calculate  $T_{max}^{set}$ .

To have  $\bar{t}_1 > 0$ ,  $\tau_{cl}^* < \tau_{cl} < \infty$  is required. The sufficient condition for it is  $F_1(\tau_{cl}^*) F_1(\infty) < 0$ . When  $\tau_{cl} \rightarrow \infty$ , we have  $\bar{t}_1 = \bar{t}_2 = \bar{t}_c \rightarrow \infty$ , and hence  $F_1(\infty) \rightarrow \Delta T > 0$ . So the sufficient condition reduced to  $F_1(\tau_{cl}^*) < 0$ .

Compared to the set-point profile, the temperature trajectory obtained in the proposed PI control system is delayed by a period of  $\tau_{cl}$ . Therefore, the set-point should be given a time of  $\tau_{cl}$  before the desired temperature trajectory.

### 3.2 Design of $PI^2D$ Control System

By applying internal model control (IMC) (Morari, 1989) principal to the first order process of (3) for dealing with a

type-2 (or ramp) input signal, an equivalent feedback controller, PI<sup>2</sup>D, can be obtained:

$$G_c(s) = \frac{1}{K} \frac{(\tau s + 1)(2\tau_f s + 1)}{\tau_f^2 s^2} \quad (17)$$

where  $\tau_f$  is a tuning parameter that determines the speed of the closed-loop response. By the final value theory, there will be no control error offset at steady-state. A sketch of the close loop response of PI<sup>2</sup>D control structure is illustrated in Fig. 5. Again, similar coordinate transformation is applied, and also assume that the process has reached the steady-state before the rising temperature reaching  $T_{ref}$ . Thus, in the ramp-up period, the temperature is just exactly the same as set-point, and  $T_p = T_{max}^{set}$ . In the ramp-down period ( $\bar{t} \geq 0$ ), we have  $\bar{T}^{set}(\bar{t}) = -k_2 \bar{t}$ , and the temperature response can be derived from the Laplace inversion of  $\bar{T}(s)$ , with two initial conditions  $\bar{T}(0) = 0$  and  $\bar{T}'(0) = k_1$ :

$$\bar{T}(\bar{t}) = L^{-1} \{ \bar{T}(s) \} = (k_1 + k_2) \bar{t} e^{-\bar{t}/\tau_f} - k_2 \bar{t} \quad (18)$$

With (18), the maximum temperature occurs at  $\bar{t}_c$  which can be obtained by

$$\frac{d\bar{T}(\bar{t})}{d\bar{t}} = (k_1 + k_2) e^{-\bar{t}/\tau_f} \left( 1 - \frac{\bar{t}}{\tau_f} \right) - k_2 = 0 \quad (19)$$

Or,  $\bar{t}_c$  can be solved as

$$\bar{t}_c = \tau_f \left[ 1 - W \left( \frac{k_2}{k_1 + k_2} \exp(1) \right) \right] = \tau_f \phi \quad (20)$$

where  $W(\bullet)$  denotes the Lambert W-function (Corless *et al.*, 1996) and

$$\phi = 1 - W \left( \frac{k_2}{k_1 + k_2} \exp(1) \right) \quad (21)$$

Thus, the maximum temperature is found as

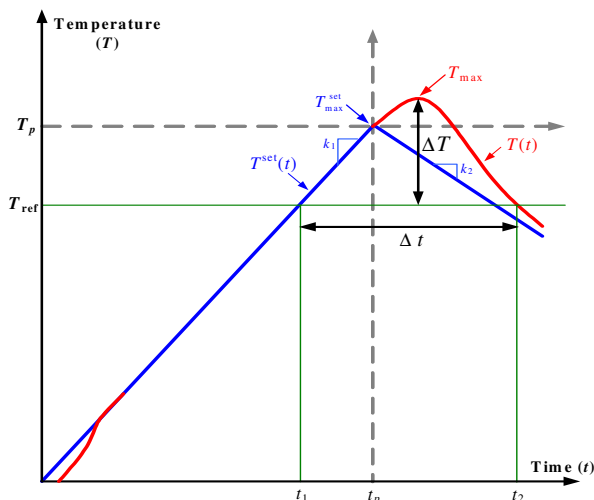


Fig. 5. Closed-loop response using PI<sup>2</sup>D controller (Dashed line represents the transformed coordinate).

$$\bar{T}_{max} = \bar{T}(\bar{t}_c) = (k_1 + k_2) \tau_f \phi e^{-\phi} - k_2 \tau_f \phi \quad (22)$$

The temperature response first intersects the reference temperature at  $\bar{t}_1$ . For  $\bar{t}_1 \leq 0$ , it can be computed by (9). For  $\bar{t}_1 > 0$ , the following equation for  $\bar{t}_1$  holds.

$$\bar{T}(\bar{t}_1) - \bar{T}_{ref} = (k_1 + k_2) \bar{t}_1 e^{-\bar{t}_1/\tau_f} - k_2 \bar{t}_1 - \bar{T}_{ref} = 0 \quad (23)$$

Furthermore,  $\bar{t}_2$  can be found by  $\bar{T}(\bar{t})$  intersecting  $\bar{T}_{ref}$ :

$$\bar{T}(\bar{t}_2) - \bar{T}_{ref} = (k_1 + k_2) \bar{t}_2 e^{-\bar{t}_2/\tau_f} - k_2 \bar{t}_2 - \bar{T}_{ref} = 0 \quad (24)$$

Like the case of PI control, by given  $k_1$  and  $k_2$ , one can tune the controller parameter,  $\tau_f$ , and design  $T_p$  (or  $T_{max}^{set}$ ) to satisfy both specifications of  $\Delta t$  and  $\Delta T$ .

Also, two cases for  $\bar{t}_1$  are discussed as follows.

**Case 1:**  $\bar{t}_1 \leq 0$ .

First, by substituting (9), (12), (13), and (22) into (24), a nonlinear equation for  $\tau_f$  is resulted. After solving for  $\tau_f$ ,  $T_{max}^{set}$  is calculated by  $T_{max}^{set} = T_p = T_{ref} + \Delta T - \bar{T}_{max}$ .

In the limiting condition of  $\bar{t}_1 = 0$ , we have  $\bar{T}_{ref} = 0$  and  $\bar{T}_{max} = \Delta T$ . Therefore, the value of  $\tau_f$  in this limiting case can be found from (22) as

$$\tau_f^* = \frac{\Delta T}{(k_1 + k_2) \phi e^{-\phi} - k_2 \phi} \quad (25)$$

As a result,  $0 < \tau_f < \tau_f^*$  is necessary to have  $\bar{t}_1 \leq 0$ . For (24) having a solution in the interval  $0 < \tau_f < \tau_f^*$ , the sufficient condition is  $F_2(0) F_2(\tau_f^*) < 0$ , where

$$F_2(\tau_f) = (k_1 + k_2) (\bar{t}_1 + \Delta t) e^{-(\bar{t}_1 + \Delta t)/\tau_f} - k_2 (\bar{t}_1 + \Delta t) - (\bar{T}_{max} - \Delta T) \quad (26)$$

**Case 2:**  $\bar{t}_1 > 0$ .

The procedure is similar to the previous case except the calculation of  $\bar{t}_1$ . By combining (23) and (24),  $\bar{t}_1$  can be solved as:

$$\bar{t}_1 = \frac{\tau_f W(\alpha) - \tau_f W(\alpha) e^{\Delta t/\tau_f} + \Delta t}{e^{\Delta t/\tau_f} - 1} \quad (27)$$

where

$$\alpha = \frac{k_2 \Delta t \exp \left( \frac{\Delta t}{\tau_f} + \frac{\Delta t}{\tau_f (e^{\Delta t/\tau_f} - 1)} \right)}{\tau_f (e^{\Delta t/\tau_f} - 1)} \quad (28)$$

Substitute (12), (13), (22) and (27) into (24) to solve  $\tau_f$ , and then  $T_{max}^{set}$  can be calculated.

To have  $\bar{t}_1 > 0$ ,  $\tau_f^* < \tau_f < \infty$  is required. Its sufficient condition is  $F_2(\tau_f^*)F_2(\infty) < 0$ . When  $\tau_f \rightarrow \infty$ , we have  $\bar{t}_1 = \bar{t}_2 = \bar{t}_c \rightarrow \infty$ , and hence  $F_2(\infty) \rightarrow \Delta T > 0$ . So the sufficient condition reduced to  $F_2(\tau_f^*) < 0$ .

#### 4. SIMULATION EXAMPLE

Consider the following first-order model for RTP system.

$$G_p(s) = \frac{4}{6s+1} \quad (29)$$

The process conditions are given as: the ramp-up rate  $k_1=150^\circ\text{C}/\text{sec}$ , the ramp-down rate  $k_2=40^\circ\text{C}/\text{sec}$ , and the reference temperature  $T_{\text{ref}}=1000^\circ\text{C}$ . The control targets are set as  $\Delta t=2$  sec and  $\Delta T=50^\circ\text{C}$ .

##### 4.1 Nominal Condition

For these control targets, the feasibility ranges on  $k_1$  and  $k_2$  for PI and PI<sup>2</sup>D control systems are first constructed based on the sufficient conditions derived in the previous section. The result is shown in Fig. 6. It can be seen that the proposed method has a wide feasibility range on  $k_1$  and  $k_2$  by tuning  $\tau_{cl}$  or  $\tau_f$ . Nevertheless, PI control system has a wider feasibility range for  $\bar{t}_1 \leq 0$  than PI<sup>2</sup>D control system.

Under the given values of  $k_1$  and  $k_2$ , Fig. 6 shows that both PI and PI<sup>2</sup>D controllers can be used to achieve the targets with  $\bar{t}_1 \leq 0$ . For PI controller, the parameter  $\tau_i$  is set as  $\tau_i = \tau = 6$ . Then, by the proposed method,  $\tau_{cl} = 0.211$  (or  $K_C=7.10$ )

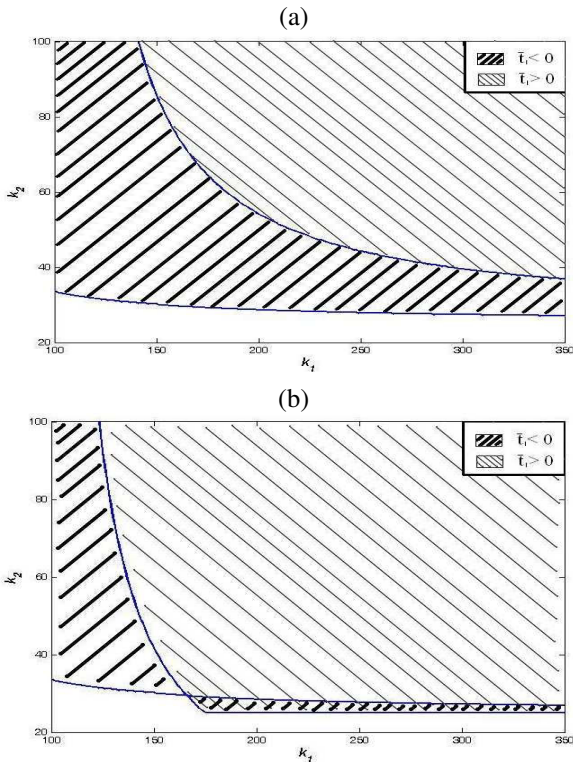


Fig. 6. Feasibility ranges on  $k_1$  and  $k_2$  for  $\Delta t=2$  sec and  $\Delta T=50^\circ\text{C}$ . (a) PI control (b) PI<sup>2</sup>D control.

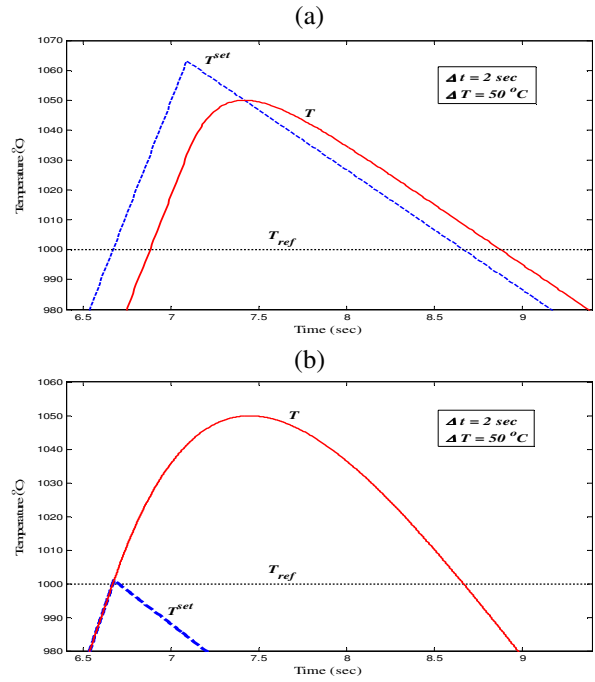


Fig. 7. Control results. (a) PI (b) PI<sup>2</sup>D controller.

and  $T_{\text{max}}^{set}=1063^\circ\text{C}$  are resulted to hit two control targets. The set-point and temperature trajectories are as shown in Fig. 7(a). For PI<sup>2</sup>D controller, the control specifications are achieved by tuning  $\tau_f = 1.267$  and  $T_{\text{max}}^{set}=1001^\circ\text{C}$ . The control result is shown in Fig. 7(b).

##### 4.2 Effect of Modelling Error

In case of process-model mismatch, the control specifications cannot be exactly achieved. Here, the effect of model mismatch is investigated through simulations. The errors of  $\Delta t$  and  $\Delta T$  under different values of model mismatch for PI and PI<sup>2</sup>D control systems are shown in Fig. 8. It can be seen that the effect of modelling error for PI<sup>2</sup>D control is greater than that for PI control, which indicates PI control system is a more robust one.

It is interesting to note that the feasibility regions of PI<sup>2</sup>D

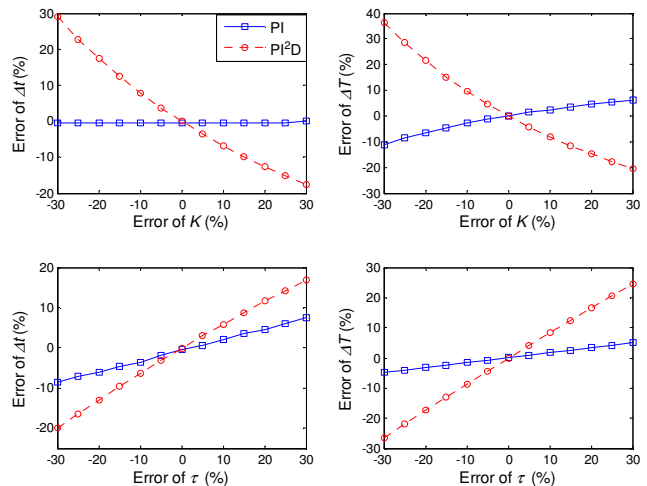


Fig. 8. Effect of model mismatch for PI and PI<sup>2</sup>D controller.

control system in Fig. 6(b) for  $\bar{t}_1 \leq 0$  and  $\bar{t}_1 > 0$  are overlapped, which implies the control specifications can be achieved with two different control designs. To compare these two control results,  $k_1=180^\circ\text{C}/\text{sec}$  and  $k_2=28^\circ\text{C}/\text{sec}$  are selected for demonstration. The calculated parameters are  $\tau_f = 0.029$  and  $T_{\max}^{set} = 1048.5^\circ\text{C}$  for  $\bar{t}_1 \leq 0$ , and  $\tau_f = 1.078$  and  $T_{\max}^{set} = 993.1^\circ\text{C}$  for  $\bar{t}_1 > 0$ . The control result is shown in Fig. 9. Although the shapes of these two temperature trajectories are quite different, the control specifications are exactly achieved in both cases. When there is modelling error, the errors of  $\Delta t$  and  $\Delta T$  under different values of model mismatch are shown in Fig. 10. The effect of modelling error in the case of  $\tau_f = 0.029$  is quite small compared to that of  $\tau_f = 1.078$ . Note that the system with more aggressive tuning (smaller  $\tau_f$ ) not only can follow the set-point well, but also exhibit good robustness. According to this result, a smaller value of  $\tau_f$  should be designed when the ramp-up/down rates fall into this region.

## 5. CONCLUSIONS

Since the RTP system has a very high system momentum, targeting perfect servo control is almost unachievable. When the control structure reaches its limitation, balancing design and control of the system is a feasible solution. In this study, we show the method for targeting thermal budget specification by designing controller and set-point profile. It comes out that the simple PI controller performs better compared to PI<sup>2</sup>D controller in the aspects of feasible range on temperature ramp-up/down rate and system robustness.

In practice, the heating process is highly nonlinear and the

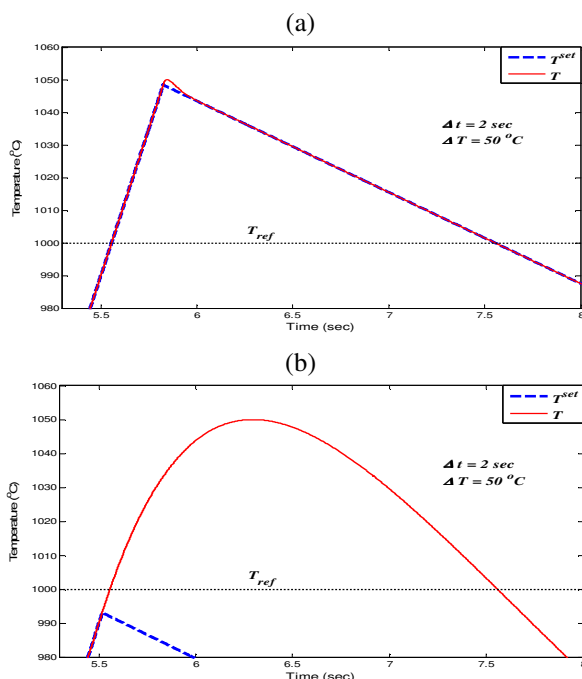


Fig. 9. Control results using PI<sup>2</sup>D controller. (a)  $\tau_f = 0.029$   
(b)  $\tau_f = 1.078$

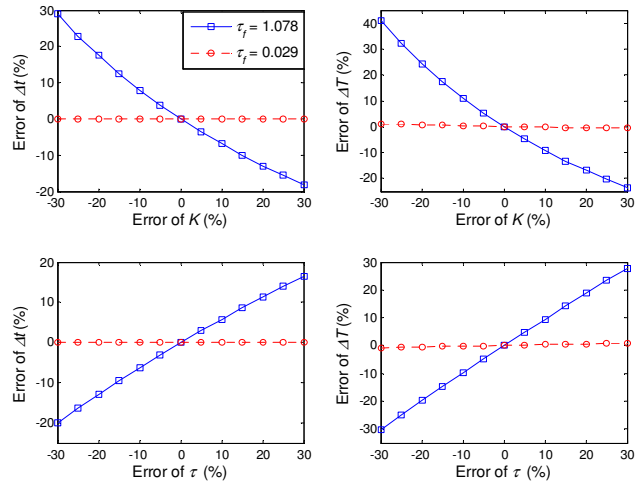


Fig. 10. Effect of model mismatch for different tuning of PI<sup>2</sup>D controller.

wafer temperature uniformity is also a very important specification. To achieve good temperature uniformity within wafer, nonlinear multivariable control strategies have to be developed. The proposed method in this paper has the potential for such an extension which are under research.

## REFERENCES

- Balakrishnan, K. S. and Edgar, T. F. (2000). Model-based control in rapid thermal processing. *Thin Solid Films*, 365, 322-333.
- Cho, M., Lee, Y., Joo, S., and Lee, K. S. (2005). Semi-empirical model-based multivariable iterative learning control of an RTP system. *IEEE Trans. Semicond. Manuf.*, 18, 430-439.
- Corless, R. M., Gonnet, G. H., Hare, D. E. G., Jerey, D. J., and Knuth, D. E. (1996). On the Lambert W function. *Adv. Computational Maths*, 5, 329-359.
- Dassau, E., Grosman, B., and Lewin, D. R. (2006). Modeling and temperature control of rapid thermal processing. *Comput. Chem. Eng.*, 30, 686-697.
- Edgar, T. F., Butler, S. W., Campbell, W. J., Pfeiffer, C., Bode, C., Hwang, S. B., Balakrishnan, K. S., and Hahn, J., (2000). Automatic control in microelectronics manufacturing: Practices, challenges, and possibilities. *Automatica*, 36, 1567-1603.
- Emami-Naeini, A., Ebert, J. L., de Roover, D., Kosut, R. L., Dettori, M., Porter, L. M., and Ghosal, S. (2003). Modeling and control of distributed thermal systems. *IEEE Trans. Contr. Syst. Techn.*, 11, 668-683.
- Huang, C. J., Yu, C. C., and Shen, S. H., (2000). Selection of measurement location for the control of rapid thermal processor. *Automatica*, 36, 705-715.
- Jung, M. Y. L., Gunawan, R., Braatz, R. D., and Seebauer, E. G. (2003). Ramp-rate effect on transient enhanced diffusion and dopant activation. *J. Electrochemical Society*, 150, G838-G842.
- Morari, M. and Zafiriou, E. (1989). *Robust Process Control*. Prentice-Hall Inc., NJ.
- Schaper, C., Cho, Y., and Kailath, T. (1992). Low-order modeling and dynamic characterization of rapid thermal processing. *Appl. Phys. A*, 54, 317-326.